DAMAGE IDENTIFICATION IN CREEP OF ALUMINIUM ALLOY 2650-T8

A. DJAKOVIC[1], B. F. DYSON[2] AND M. MCLEAN[2]

*[1]YU POINT DOO, Francuska 6, 11000 Belgrade, Serbia and Montenegro,
a_djakovic@yahoo.com , alex@eph.point-group.com, [2]Department of Materials,
Imperial College London, Exhibition Road, SW7 2BP, UK*

ABSTRACT

Constant-load creep tests were performed for aluminium alloy 2650-T8 giving creep rupture lives from ~10 to ~6,500 hours at 423K (150°C) and 448K (175°C). The response of the alloy during creep testing is related to the microstructure that is evolving. The creep behaviour of the alloy is explained by the concepts of damage processes which through their evolution control the acceleration of the creep strain accumulation. Specialised creep tests were performed to examine the validity of the damage mechanisms.

Key words: aluminium alloy 2650-T8, aerospace, Concorde, creep, damage, microstructure evolution, precipitate coarsening, dislocation multiplication, grain boundary cavitation, cavity growth

INTRODUCTION

During creep, different materials exhibit different microstructural changes which can influence the creep performance of an engineering component. Even though a number of alloys exhibit a common creep curve shape in tension (suggests a common mechanism), these similar creep curve shapes can be caused by quite different damage mechanisms and thus, different materials cannot be effectively represented by a universal creep equation. It is fundamental for the constitutive laws used in the creep predictive models to reflect the controlling creep mechanism(s). It is essential to establish the controlling damage mechanism(s) in an engineering alloy and to explicitly consider the corresponding microstructural changes, and incorporate them in the main constitutive laws and state variables of a predictive model, allowing all micromechanisms to interact with each other and microstructural variables to evolve with time.

Aluminium alloys for high-temperature airframes have been the aerospace development research topic for several decades. Aluminium alloy (precipitate-strengthened) 2650-T8 investigated in this work is a candidate fuselage material for the future supersonic transport and is a modification of the current Concorde aluminium alloy 2618. The work presented here attempts to clearly identify the operating damage mechanisms and qualitatively establish their importance/dominance under different loading conditions during creep of the alloy 2650-T8.

EXPERIMENTAL

In the T8 state the 2650 alloy has been solution heat treated at 506°C for 1 hour, room temperature water quenched, 0.8% pre-strained and artificially (peak) aged for 19 hours at 190°C, producing a fine dispersion of needle or rod-shape S'/S precipitate particles in the α-matrix. The peak-aged material was supplied by Aerospatiale Matra in the form of 6mm thick sheet and its composition (weight %) is given in Table 1, alongside that of the current Concorde alloy 2618. The term "as-received" is used hereafter to describe the alloy in the peak-aged condition.

Table 1.Composition of alloys 2650/2618 (weight %), as supplied by Aerospatiale Matra

Alloy	Cu	Mg	Mn	Cr	Si	Fe	Ni	Ti	Zn	Zr
2650	2.71	1.64	0.34	0.01	0.21	0.20	0.21	0.10	0.04	0.02
2618	2.59	1.60	0.09	0.01	0.22	1.04	1.14	0.08	0.04	

Mechanical testing. All creep tests in both tension and compression have been performed at IncoTest Special Metals Wiggin Ltd, Hereford, UK according to BS EN 10291 (2000) and ASTM E139 standards. Tensile test-pieces were machined according to standard BS 3500 (1969) having a 6mm × 6mm cross-section. Compression test-pieces were machined to have the height of 12mm and the same square cross-section. 2650-T8 samples were artificially overaged in an air-circulating furnace for 1, 5, 10, 50, 100, 200, 500, 1000 and 2000 hours at 150°C, 165°C, 175°C and 182°C (±1°C) with their hardness H_v measured.

Electron microscopy. Transmission Electron Microscopy (TEM) was employed in investigating the precipitate microstructure and potential damages due to coarsening and dislocation multiplication. Scanning Electron Microscopy (SEM) was applied in examining the microstructure of the as-received and crept material. Software called "UTHSCSA Image Tool for Windows Version 3.00" was used for the quantitative analyses of the TEM and SEM images.

RESULTS OF MECHANICAL TESTING

Tensile creep of as-received 2650-T8. Results of the creep tests performed in this work on the 6mm thick material (marked as "present work") are shown along with data supplied by the companies Aerospatiale Matra and Onera (marked as "others") [1], which are for the thin 1.6mm plate section of the alloy. The only difference between the two is the grain size e.g. ~30μm in the thin and ~40μm in the thick section material (examined here) in the RD direction. All creep tests presented here were performed in tension, unless otherwise stated.

Fig. 1 shows the global creep behaviour of the alloy 2650-T8 at 175°C, 150°C and 130°C (stress against time to rupture and minimum creep rate against stress). It can be seen that the thick section appears to have somewhat better creep behaviour below 250MPa at 175°C and the difference is smaller at 150°C, only becoming notable below ~220MPa (e.g. at 200MPa, thin section alloy failed in ~10,760h and the thick section alloy reached only 0.41% after ~9,000h). The above observation indicates that the grain

size does influence the creep behaviour of the alloy, having a larger effect at 175°C than at 150°C and this means that the main difference between the creep responses of the two section sizes is the extent of grain boundary damage. Thick section material with bigger grain size was found to have higher strains at rupture, also suggesting that the possible difference is in the extent of grain boundary damage i.e. cavitation. The thicker alloy displayed rupture strains of approximately 7-11%, while the thinner showed 2-6%. It can also be clearly seen in Fig. 1 that the minimum creep rates are not linearly related to the stress in the Log-Log plots. This means a variable stress exponent n from the Power Law (here found to vary from ~40 to ~6), showing the core problem of this empirical function. The data presented hereafter is the data obtained in the present work for the thick section material, unless otherwise stated.
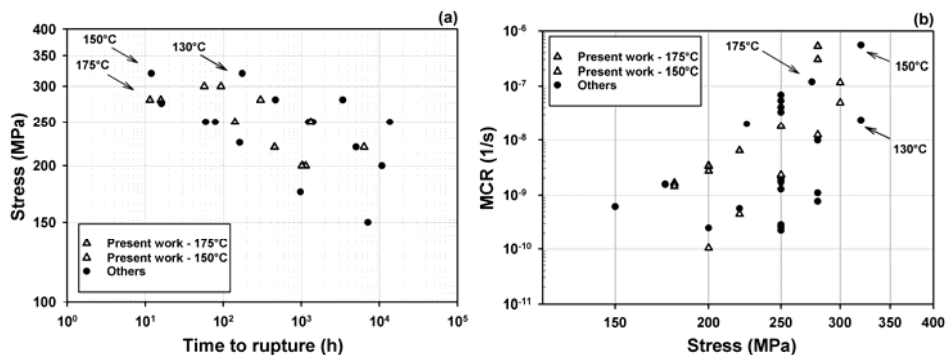

Fig. 1. Global creep behaviour of the alloy 2650-T8 at 175°C, 150°C and 130°C:
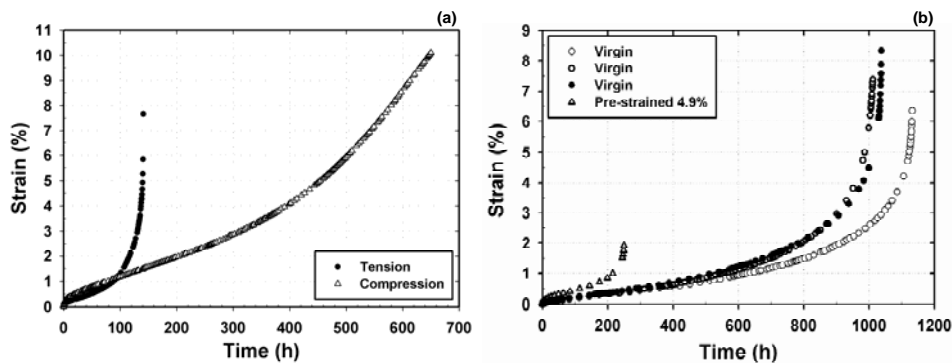(a) stress against time to rupture and (b) minimum creep rate against stress

Fig. 2. (a) tension/compression asymmetry in creep at 250MPa and 175°C; (b) effect of
4.9% cold pre-straining prior to creep at 200MPa and 175°C

Tension/compression asymmetry. Fig. 2 (a) shows the comparison between the tension and compression creep of the as-received 2650-T8. Primary creep rates could indicate the presence of a residual internal stress. A slight curve asymmetry is expected due to the different effect of constant load testing in tension and in compression; however, such asymmetry can only be explained by the concept of grain boundary cavity growth, where compression does not allow the cavity growth on the grain boundaries perpendicular to the stress axis. Compression creep also clearly shows the presence of

tertiary creep acceleration. This evidently shows that some damage does operate even in compression.

The effect of pre-strain prior to creep. A sample was 4.9% plastically pre-strained cold and then crept at 200MPa and 175°C; see Fig. 2 (b), where creep of the pre-strained material is compared to that of the virgin (as-received). Initial strain rate and minimum creep rate are clearly higher in the pre-strained material proving that prior pre-strain has an overall accelerating effect on creep rates. The most noticeable effects are the much smaller lifetime and strain to rupture (both by a factor of 5), attributable to an extensive grain boundary cavitation damage due to plastic pre-straining.

The effect of overageing prior to creep. Four test-pieces were given the same overageing treatment - 2,000h at 182°C and were examined in creep at 150°C under 280MPa, 265MPa, 250MPa and 235MPa. Fig. 3 compares one of the overaged creep tests with the corresponding one of the virgin material at 250MPa at 150°C. Initial and minimum creep rates and generally strain rates throughout the creep curve are much higher for the overaged material and the time to rupture is much reduced (the precipitate function in the creep mechanism has diminished significantly). It was found that the creep behaviour of the overaged material approaches that of the virgin as stress level drops (converging towards the low stress regime), as can be expected since the initial damage due to precipitate size growth has the most drastic effect in the high stress tests, where very little thermal damage takes place in the virgin material.
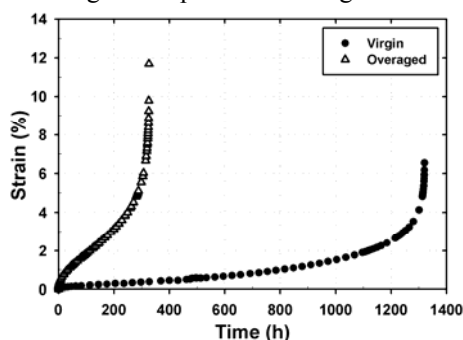

Fig. 3. Effect of overageing prior to creep at 250MPa and 150°C.

MATERIAL CHARACTERISATION

As-received virgin alloy microstructure. The presence of the needle- or rod-shape S'/S precipitate particles (Al_2CuMg) imparts the creep strength to the alloy by behaving as obstacles to dislocations. In this work it is not implied that S' and S are the same or distinct phases. The grains were found to be on average 42μm, 31μm and 28μm in RD, LT and ST directions respectively (linear intercept method). Al_9FeNi particles were found by EDX inside the grains and on their boundaries. The typical orthogonal orientation of the S'/S precipitates along the crystal cube directions was found by TEM in Fig. 4, where it can be seen that the S'/S particles have also nucleated on dislocation lines. Some very small particles can also be seen in Fig. 4(a) (appear to be homogeneously nucleated particles), but they are not characterised here because they disappear on a very short ageing at T_{ageing}>150°C (thought to dissolve at the expense of S'/S growth). It is not argued here if these particles are GPB2, S'' or S'. The volume

fraction of the (heterogeneous) S'/S precipitate particles was estimated from the TEM images by using the measured average rod radius (~4nm) and rod length (~150nm), as was the volume fraction of Fe/Ni rich intermetallic particles (volume fraction approximated by the area fraction) from SEM images; see Table 2.

Table 2. Volume fractions of the S'/S precipitate and Fe/Ni rich intermetallic particles

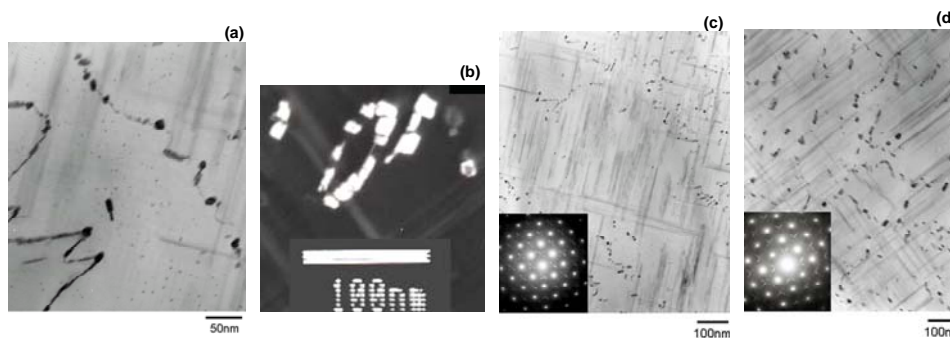| S'/S precipitate particles	Fe/Ni rich intermetallics e.g. Al$_9$FeNi
$3.01 \begin{smallmatrix} +0.54 \\ -0.82 \end{smallmatrix}$ %	$1.30 \begin{smallmatrix} +0.20 \\ -0.40 \end{smallmatrix}$ %

Fig. 4. TEM images of the S'/S precipitate microstructure in [001] zone: (a) BF,
(b) DF and (c) BF images of as-received material;
(d) BF image of 2,000h overaged material at 182°C

Precipitate coarsening. Coarsening of the S'/S precipitate particles is a proposed damage mechanism during high temperature creep and was analysed following an overageing study of the as-received samples at 150°C, 165°C, 175°C and 182°C. Fig. 4(d) and Fig. 5 show the overageing effect on the alloy microstructure and Vickers hardness (rod-shape particles were assumed to have the length L and to be elliptical in cross-section). The particles have grown laterally and longitudinally and there is a coarser dispersion after overageing.
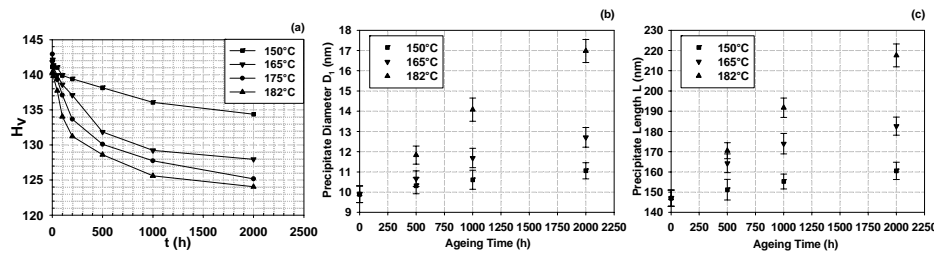

Fig. 5. Overageing effect on (a) Vickers hardness (b) D_1 – larger diameter, (c) L - length

A modified Lifshitz, Slyozov and Wagner (LSW) equation is used to calculate the S'/S coarsening kinetics [2]. The surface curvature of both cylindrical and spherical particles is inversely proportional to the particle radius, but the coarsening rate constant

k is different due to the different curvature constant (shape factor is 8/9 for spheres and 0.47 for cylinders or rods). The LSW equation hence becomes:

$$r^3 - r_0^3 = \frac{0.47\, D\gamma V_m C_\alpha}{RT} t \quad k = \frac{0.47\, D\gamma V_m C_\alpha}{RT} \quad k = k_0 \exp\left(-\left(\frac{Q_c}{RT}\right)\right) \tag{1}$$

where r is the average particle radius (r_0 at time t=0), D is the volume diffusion coefficient of the diffusing species, γ is the specific surface free energy of the particle/matrix interface, V_m the molar volume of the precipitate, C_α the equilibrium solute content in the matrix, R the gas constant, T the temperature (in K), k_0 a material constant and Q_c is the coarsening activation energy. An equivalent sphere coarsening kinetics can be calculated by collapsing a rod precipitate to an equivalent spherical precipitate, but this approximation procedure invariably leads to large misinterpretation of the coarsening kinetics of rod-like particles. Using the data in Fig. 5, average coarsening activation energy Q_c and material constant k_0 were calculated to be $Q_c = 122$ kJ/mol and $k_0 = 1.78 \times 10^{-18}$ m^3/s.

Dislocation multiplication. In Fig. 6, as-received sample is compared to the sample that crept at 220MPa and 150°C. Increased number of dislocations can be clearly seen in the crept sample, showing that mobile dislocation multiplication is operating as a damage mechanism in the alloy. Dislocation density was estimated from TEM images by measuring the total visible dislocation line length and dividing it by the volume of the material (assuming the foil thickness of ~150nm). Each studied section was rotated and tilted by 45° in order to ensure all dislocation lines within the section were observed. The results obtained were $(6.34\pm1.45)\times10^{13}$ m^{-2} for the as-received sample and $(1.16\pm0.25)\times10^{14}$ m^{-2} for the sample that crept at 220MPa and 150°C.
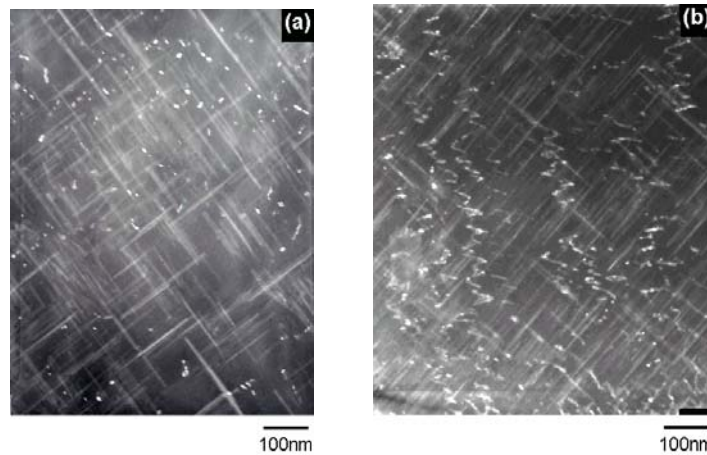

Fig. 6. [001] zone DF images (a) as-received (b) crept at 220MPa and 150°C with a strain to rupture of 7.99%.

Grain boundary cavity growth. This damage has been reported to occur in polycrystalline materials in creep [3,4] and to depend strongly on the alloy state (e.g. level of pre-straining, heat-treatment, physical properties) and the testing conditions

(expected to be more pronounced at higher temperature as grain boundary vacancy diffusivities increase).

The creep fracture surface (200MPa 175°C) of the virgin material showed a partially ductile failure, while that of the 4.9% pre-strained material displayed a typical intergranular fracture with a clear grain structure outline (indicating extensive grain boundary damage). Cavities of the order of 1μm were revealed by SEM on the grain boundaries of the crept virgin sample (creep cavity size usually reported [5,6]). However, an unambiguous conclusion cannot be made due to the small number of the observed cavities and the possibility that they could actually be artefacts of the etchant.

In the crept pre-strained sample, many grain boundary submicron creep cavities were found, some at the sites of grain boundary particles. Some of these particles were found situated inside the cavities; see Fig. 7. This may indicate that these particles act as nucleation sites for creep cavities. The EDX analysis of these particles showed that they belong to the Al-Cu-Mg system (most likely Al_2CuMg i.e. S phase). This is contrary to the claim in [1] that the Fe/Ni intermetallic particles (much larger) act as the nucleation sites.
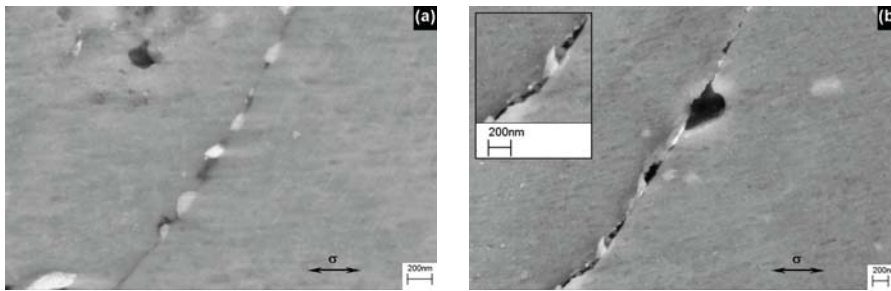

Fig. 7. 4.9% pre-strained test-piece crept at 200MPa and 175°C: (a) submicron size cavities on a grain boundary nucleated at the sites of grain boundary particles, (b) grain boundary particles revealed inside the cavities.

CONCLUSIONS

Dislocation multiplication, particle coarsening and grain boundary cavity growth were found to be the possible creep damage mechanisms operating in the aluminium alloy 2650-T8. During overageing, S'/S precipitate particles grew laterally and longitudinally and the as-received material softened significantly, inducing much higher creep strain rates. TEM showed that dislocations are being generated during creep, with the dislocation density significantly increasing during creep. SEM investigation of the crept samples is inconclusive in indicating whether the cavity growth is present as a dominant damage mechanism in the virgin material, but it is clearly identified to be present as such in the pre-strained material. Compression creep tests clearly showed the presence of accelerating tertiary creep, demonstrating that damage evolution is present in compression.

ACKNOWLEDGMENTS

REFERENCES

[1] J.Przydatek, The Elevated Temperature Deformation of Aluminium Alloy 2650, Ph.D. Thesis, Department of Materials, Imperial College London (1998).

[2] M.McLean, *Directionally Solidified Materials for High temperature Service*, Predictive and Quantitative Metallurgy Series (1983) The Metals Society, London.

[3] B.F.Dyson and M.McLean, Microstructural Stability of Creep Resistant Alloys for High Temperature Plant Applications (number 2), edited by A.Strang, J.Cawley and G.W.Greenwood, The Institute of Materials, London (1998), pp.371-393.

[4] B.F.Dyson, *Modelling Creep Rupture Ductilities and Lifetimes in a Commercial Aluminium Alloy*, in Creep Deformation: Fundamentals and Applications, edited by R.S.Mishra, J.C.Earthman and S.V.Raj, pp.309-318, proceedings of 2002 TMS Annual Meeting and Exhibition, Seattle, Washington, February 17-21, 2002.

[5] B.F.Dyson and M.J.Rodgers, *Pre-strain, Cavitation and Creep Ductility*, Metal Science **8** (1974) pp. 261-266.

[6] R.K.Varma and B.F.Dyson, *Metallographic Detection of Atom-Plating due to Cavity Growth*, Scripta Metall. **16** (1982) pp. 1279-1284.